Published in final edited form as:

J Comp Neurol. 2013 October 15; 521(15): 3570–3583. doi:10.1002/cne.23372.

Subcellular Organization of CaMKII in Rat Hippocampal Pyramidal Neurons

Jin-Dong Ding[1,*], **Mary B. Kennedy**[2], and **Richard J. Weinberg**[3]

[1]Department of Ophthalmology, Duke University Medical Center, Durham, North Carolina 27710

[2]Department of Biology, California Institute of Technology, Pasadena, California 91125

[3]Department of Cell Biology and Physiology, and Neuroscience Center, University of North Carolina, Chapel Hill, North Carolina 27599

Abstract

Calcium/calmodulin-dependent protein kinase II (CaM-KII) plays a key role in *N*-methyl-D-aspartate (NMDA) receptor-dependent long-term synaptic plasticity; its location is critical for signal transduction, and may provide clues that further elucidate its function. We therefore examined the subcellular localization of CaMKII in CA1 stratum radiatum of adult rat hippocampus, by using immuno-electron microscopy after chemical fixation. When tissue was fixed quickly, the concentration of CaMKIIα (assessed by pre-embedding immunogold) was significantly higher in dendritic shafts than in spine heads. However, when tissue was fixed 5 minutes after perfusion with normal saline, the density of labeling decreased in dendritic shaft while increasing in spine heads, implying rapid translocation into the spine during brief perimortem stress. Likewise, in quickly fixed tissue, CaMKII within spine heads was found at comparable concentrations in the “proximal” half (adjacent to the spine neck) and the “distal” half (containing the postsynaptic density [PSD]), whereas after delayed fixation, label density increased in the distal side of the spine head, suggesting that CaMKII within the spine head moves toward the PSD during this interval. To estimate its distribution at the synapse *in vivo*, we performed postembedding immunogold staining for CaMKII in quick-fixed tissue, and found that the enzyme did not concentrate primarily within the central matrix of the PSD. Instead, labeling density peaked ∼40 nm inside the postsynaptic membrane, at the cytoplasmic fringe of the PSD. Labeling within 25 nm of the postsynaptic membrane concentrated at the lateral edge of the synapse. This lateral “PSD core” pool of CaMKII may play a special role in synaptic plasticity.

*Correspondence to: Jin-Dong Ding, Department of Ophthalmology, Duke University Medical Center, PO Box 3802, 2351 Erwin Rd., Durham, NC, 27710. jdding@gmail.com.

Additional Supplementary Material may be found in the online version of this article.

Conflict of Interest Statement: The authors declare there is no conflict of interest.

Role Of Authors: All authors had full access to all the data in the study and take responsibility for the integrity of the data and the accuracy of the data analysis. Study concept and design: RJW, JDD, and MBK. Acquisition and analysis of data: JDD and RJW. Interpretation of data: JDD, MBK, and RJW. Drafting of the manuscript: JDD and RJW. Obtained funding to support the research: MBK and RJW.

Indexing Terms

immunogold electron microscopy; synaptic plasticity; postsynaptic density; hypoxia

Calcium/calmodulin-dependent protein kinase II (CaMKII), a holomeric enzyme of ∼600 kDa comprising 12 subunits, is one of the most abundant proteins in the brain (Bennett et al., 1983; Kennedy et al., 1983; Erondu and Kennedy, 1985). In the hippocampus, it is selectively expressed by excitatory neurons (Sik et al., 1998). This calcium-dependent enzyme can autophos-phorylate to become constitutively active, thus serving as a "molecular switch" that responds to brief [Ca^{2+}] transients with sustained activity (Soderling, 2000). Acting downstream of the *N*-methyl-D-aspartate (NMDA) receptor, CaMKII plays a crucial role in long-term potentiation (LTP) in the CA1 field of hippocampus (Lledo et al., 1995; Lisman et al., 2002, 2012), at least in part via phosphorylation of the α-amino-3-hydroxy-5-methyl-4-isoxazolepropionic acid (AMPA) receptor (Barria et al., 1997). CaMKII might also play a direct role in cytoskeletal reorganization by bundling F-actin filaments (Okamoto et al., 2007; Honkura et al., 2008), which may mediate the spine enlargement associated with LTP.

The location of CaMKII is crucial for its function (Barria and Malinow, 2005; Lee et al., 2009; Halt et al., 2012). However, despite considerable work addressing its subcellular location, methodological limitations may have led to misleading conclusions. Hypoxic/ischemic stress triggers rapid translocation of CaMKII to the synapse (Suzuki et al., 1994; Hu and Wieloch, 1995; Hu et al., 1998; Domańska-Janik et al., 1999; Chen et al., 2005), but is unavoidable during biochemical purification of the postsynaptic density (PSD) fraction. This difficulty, along with CaMKII's tendency in the presence of elevated Ca^{2+} to form large aggregates that may cofractionate with the PSD (Dosemeci et al., 2000; Tao-Cheng et al., 2002), implies that biochemical methods may overestimate its enrichment in the PSD *in vivo*.

Some degree of hypoxic/ischemic stress is also unavoidable in acute slice experiments. Live-cell imaging techniques permit direct study of CaMKII localization, but its organization in slice cultures and in cultures from disassociated neurons may also differ from that in the intact animal; moreover, the exogenous transfection of tagged CaMKII used in imaging studies may lead to distortions associated with overexpression and/or tagging. These methods also suffer from the limited spatial resolution of light microscopy.

In the present study, we have used immunogold electron microscopy to re-examine the localization of CaMKII in the hippocampus of the adult rat, taking precautions to minimize the duration of hypoxia before chemical fixation. We find that the density of CaMKIIα is higher in dendritic shafts than in spine heads. Within the head, CaMKII concentrates at the cytoplasmic fringe of the PSD, ∼40 nm away from the plasma membrane; a smaller pool within the PSD core concentrates at its lateral edge.

Materials and Methods

Animals

All procedures related to the care and treatment of animals were strictly in accordance with institutional and NIH guidelines. Sprague-Dawley rats (Charles River, Wilmington, MA) were deeply anesthetized with sodium pentobarbital (60 mg/kg, i.p.), and then perfused transcardially, flushing with normal saline either very briefly (<1 minute; "quick-fix") or for 5 minutes ("delay-fix"), immediately followed by perfusion with fixative containing a mixture of 2% freshly depolymerized paraformaldehyde and 2% glutaral-dehyde in 0.1 M phosphate buffer (PB), pH 7.4. (Perfusion solutions were at room temperature.) Brains were removed and postfixed in 4% paraformaldehyde (in PB, pH 7.4) overnight at 4 °C. Fifty-μm-thick sections containing hippocampus were cut on a Vibratome.

Characterization of the CaMKII antibodies

The primary antibody used for the pre-embedding experiments was clone 6G9, raised against the α-subunit of CaMKII (Erondu and Kennedy, 1985; Table 1). Although this antibody has been widely used, we confirmed its specificity, taking advantage of published data showing that at early postnatal days, CaMKIIα is expressed at greatly reduced levels in the hippocampus and cerebral cortex (Burgin et al., 1990; Bayer et al., 1999; Petralia et al., 2005). Brain sections from immature (postnatal days 1, 5, and 10) and adult rats were pretreated with 3% H_2O_2 for 30 minutes to quench endogenous peroxidase. Sections were then blocked for 30 minutes with 10% normal donkey serum (NDS) and incubated overnight with 6G9 antibody (1:1,000), and then in biotinylated donkey anti-mouse secondary antibody (1:200; Jackson ImmunoResearch, West Grove, PA) for 2 hours, and for 1 hour in ExtrAvidin-peroxidase complex (1:5,000; Sigma, St. Louis, MO). Peroxidase was visualized with diaminobenzidine. Processed sections were mounted on slides, dehydrated, and coverslipped. Consistent with previous reports using *in situ* hybridization, immunostaining was weak in the hippocampus, and barely detectable in the neocortex, before postnatal day 10 (Fig. 1A-C). We conclude that immunostaining with this antibody in our hands selectively detects authentic CaMKIIα protein, with little or no interference from CaMKIIβ (which is already expressed at substantial levels at birth; Burgin et al., 1990).

In contrast to its excellent performance for preembedding immunohistochemistry, postembedding immunolabeling with the 6G9 antibody was sparse; apparently the additional processing necessary for postembedding degraded the relevant epitopes. We therefore also used a second primary antibody for postembedding, EP1829Y, a rabbit monoclonal from Origene (Rockville, MD; cat. no. TA303876; Table 1), raised against a 15-amino acid sequence within amino acids 200–250 of human CaMKII. This antibody has been reported in previous publications to recognize authentic CaMKIIα protein in western blots (Lee et al., 2009); it also recognizes the CaMKIIβ isoform. To further confirm its specificity, we performed double-label immunofluorescence experiments, verifying nearly complete colocalization of EP1829Y with 6G9 within the hippocampus of the adult rat (Fig. 1D–I). Postembedding immunogold processing yielded robust and abundant synaptic label in adult cortex; labeling was much weaker in the cortex from postnatal day 10, further supporting the specificity of this antibody in our postembedding experiments.

Immunohistochemistry using pre-embedding immunogold

Brain sections from three quick-fix and three delay-fix adult rats were permeabilized with 50% ethanol for 30 minutes, and treated with 1% sodium borohydride for 30 minutes to quench free aldehyde groups. Sections were then blocked with 10% NDS for 30 minutes and incubated overnight with primary antibody (6G9 at 1:1,000), followed by biotinylated donkey anti-mouse secondary antibody (1:200) for 2 hours. Sections were then incubated for 1 hour with streptavidin-conjugated nanogold (Nanoprobe, Yaphank, NY). The gold particles were amplified with silver enhancement, by using either IntenSE (GE Healthcare, Piscataway, NJ) or R-Gent SE-EM (AURION, Wageningen, The Netherlands). Sections were postfixed with osmium, dehydrated, and embedded in a mixture of Epon and Spurr resins. Thin (∼80 nm) sections were cut from the CA1 field of the hippocampus and poststained with 1% uranyl acetate followed by Sato's lead (Sato, 1968).

Immunohistochemistry using postembedding immunogold

Brain sections cut on a Vibratome from nine quick-fix adult rats were pretreated in 0.1% $CaCl_2$ in 0.1 M sodium acetate, rinsed, and then cryoprotected in 30% glycerol in 0.1 M sodium acetate. Pieces isolated from tissue slices containing the CA1 field of the hippocampus were quick-frozen in isopentane chilled with dry ice. Freeze substitution in 4% uranyl acetate in methanol was carried out in a Leica (Deerfield, IL) Electron Microscopy Automatic Freeze Substitution System; dehydrated blocks of CA1 hippocampus were embedded in Lowicryl HM-20. Sections were cut at ∼70–90 nm with an ultramicrotome and collected on nickel grids, coated with Coat-Quick (Polysciences, Warrington, PA). Postembedding immunocytochemistry was performed as described previously (Phend et al., 1995; Kharazia and Weinberg, 1999). Briefly, grids were pretreated in 4% *p*-phenylene diamine in Tris-buffered saline or citrate buffer with 0.005% Tergitol NP-10 (Dow Chemical, Midland, MI), blocked in 1% bovine serum albumin (BSA), and then incubated overnight at room temperature in the 6G9 (1:100) or EP1829Y (1:800) antibodies. Grids were rinsed, blocked in 1% NGS, incubated in goat anti-mouse IgG $F(ab')_2$ conjugated to 10-nm gold particles (1:15; Ted Pella, Redding, CA) for 2 hours, rinsed, and then poststained with 1% uranyl acetate followed by Sato's lead (Sato, 1968).

Image acquisition and data analysis

Thin sections were viewed on a Philips Tecnai 12 transmission electron microscope (FEI, Hillsboro, OR), and images from the stratum radiatum of CA1 were collected with a cooled CCD camera (12-bit 1,024 × 1,024 pixels; Gatan, Pleasanton, CA). To compare the density of labeling in dendritic shafts and spine heads, we collected electron micrographs from the stratum radiatum that included both a parent dendrite and its spines in the same plane of section. Spine necks were identified as narrow filament-containing structures, which appear darker than neighboring shafts and spine heads. After demarcation of the spine necks (Fig. 2A–C), areas of dendritic shafts and spine heads were measured with ImageJ (NIH), allowing computation of particle density. Data were analyzed with Excel (Microsoft, Bellevue, WA) and Numbers (Apple, Cupertino, CA) spreadsheets.

For analysis of synaptic label in postembedding material, micrographs were randomly collected from spines that exhibited at least one gold particle within 150 nm of the synapse

and clearly defined synaptic membranes (suggesting a plane of section nearly orthogonal to the plane of the membrane). For "axodendritic" analysis, the distance from the center of each particle to the closest point on the plasma membrane was tabulated. To assess tangential position along the synapse, a line through each particle was drawn perpendicular to the plasma membrane, and the distances from this point on the membrane to each side of the synaptic specialization (*a* and *b*) were measured (thus, $a + b$ would represent the total length of the synapse in the plane examined). "Normalized lateral position" (defined such that 0 corresponded to the center of the synapse (a point whose projection onto the membrane lay equidistant between the two ends of the synapse), and 1 to the edge of the synapse) was computed as the absolute value of $(a - b)/(a + b)$. Graphs were prepared by using Kaleidagraph v.4.1 (Synergy Software, Reading, PA), and statistics were computed with DataDesk v.6.3 (Data Description, Ithaca, NY). Plates were composed and edited with CorelDraw (Corel, Ottawa, ON, Canada) and Photoshop (Adobe Systems, San Jose, CA). For composition, images were resized. In many cases brightness and contrast were adjusted and some images were digitally sharpened, but all digital modifications were applied uniformly to the entire image.

Results

CaMKII in dendritic shafts and spines after quick fixation

We performed immunogold labeling on tissue from quick-fix rats to estimate the subcellular distribution of CaMKII *in vivo*. Following deep pentobarbital anesthesia (which reduces both electrical and metabolic activity in brain), we rapidly exposed the heart, perfusing the aorta with fixative that likely reached the brain within ∼30 seconds after cessation of respiration, as assessed by the onset of rigor in the periphery. Using pre-embedding immunogold to assess the distribution of antigen in cytoplasm, we found labeling in both dendritic shafts and spines of CA1 pyramidal neurons (Fig. 2A). Within the shaft, CaMKIIα was found in association with various subcellular compartments, including the plasma membrane, microtubules, and mitochondria (Fig. 2B–D).

CaMKIIα labeling seemed denser in shafts than spines. To test this impression, we collected electron micrographs of CA1 pyramidal neurons that included both a parent dendrite and its spines in the same plane of section (Fig. 2A–C), thus ensuring that we compared levels of labeling from the same neighborhood of the same cell. The density of CaMKIIα labeling in the shaft was 75.1 ± 3.2 particles/μm^2 (mean ± SEM; $n = 61$ shafts), whereas the labeling density in the spine head was only 43.4 ± 5.1 particles/(μm^2 ($n = 64$ spines); labeling was significantly denser in shafts than spine heads (Fig. 2E; $P < 0.001$, two-sided *t*-test).

Prolonged saline flush causes cytoplasmic redistribution of CaMKII

Biochemical work has shown that the hypoxic/ischemic stress associated with decapitation leads to increased CaMKII in the PSD fraction (Aronowski et al., 1992; Kolb et al., 1995; Domańska-Janik et al., 1999), even if the brain is stored for only a few minutes on ice (Suzuki et al., 1994). Likewise, ischemia has been shown to modify the PSD *in vivo* (Hu and Wieloch, 1995; Hu et al., 1998; Tao-Cheng et al., 2007), but it is unclear whether hypoxic/ischemic stress also modifies the distribution of CaMKII in cytosolic compartments.

Because the issue bears on interpretation of our results from quick-fix tissue, we analyzed samples from rat hippocampus that had been fixed after a 5-minute perfusion with saline (delay-fix). Although the overall pattern of labeling (Fig. 3A) was similar to that of quick-fix tissue, characteristic electron-dense spheroids decorated with CaMKII labeling were found in the dendritic shaft of delay-fix material (Fig. 3B, arrowheads); these likely correspond to the CaMKII aggregates reported previously (Dosemeci et al., 2000). Although adequate for analysis, the ultrastructure was somewhat disrupted (note, for example, tissue "holes" visible in Fig. 3A).

Unlike in quick-fix tissue, labeling density in the delay-fix material was similar ($P > 0.1$; *t*-test) for shafts (57.4 ± 2.5 particles/μm^2; $n = 64$) and spine heads (49.7 ± 4.5 particles/μm^2; $n = 70$; Fig. 2C), reflecting both a slightly higher concentration in the spine and a substantially lower concentration in the shaft, compared with the quick-fix material. The spine head showed a modest enlargement in delay-fix tissue (mean area 0.107 ± 0.009 μm^2) compared with quick-fix (mean area 0.087 ± 0.007 μm^2). Significantly more CaMKII was detected in spine heads, as assessed by pre-embedding immunogold (3.4 ± 0.4 particles/spine head for quick fix, 4.8 ± 0.5 particles/spine head for delay fix, $P < 0.05$; Fig. 2D), implying a translocation of CaMKII from shaft to spine during the delay. This result is reminiscent of previous results from chemically-induced LTP in slice culture (Otmakhov et al., 2004); indeed, we cannot exclude the possibility that the translocation we observed was a consequence of excessive glutamate release caused by hypoxia. In any case, we conclude that CaMKII translocates into spines within 5 minutes after the onset of saline flush.

We wondered whether CaMKII also redistributed within the spine head itself following hypoxia, as suggested by qualitative examination of the material (Fig. 4A–D). To assess this possibility, we bisected the spine head into a "distal" half including the PSD, and a "proximal" half facing the parent dendrite (see diagram on right of Fig. 4E), and measured the relative distributions of CaMKIIα by computing the ratio (number of gold particles on the PSD side)/(total number of particles); a value of 0.5 would correspond to a uniform distribution. For quick-fix spine heads, CaMKII was equally distributed between the two halves (0.49 ± 0.04; = 48), but in the delay-fix spine heads, CaMKII concentrated in the "PSD half" of the spine head (0.68 ± 0.04; $n = 54$; $P < 0.001$).

Together, the above findings demonstrate a significant redistribution of CaMKIIα from the dendrite into the distal portion of the spine head after a 5-minute flush with saline. In contrast, the relatively modest magnitude of the effect suggests that the very brief hypoxic/ischemic stress associated with rapid fixation should cause minimal disruption of the in vivo organization of the protein.

Distribution of CaMKII at the synapse

The synapse itself immunolabeled only weakly with pre-embedding methods, presumably reflecting limited access of antibody to the protein-dense matrix of the PSD. To study the synaptic distribution of CaMKII, we therefore used postembedding immunogold methods, which provide high spatial resolution while avoiding problems of antibody access (because reagents have unbiased access to the entire surface of thin plastic sections, cut randomly through all tissue compartments). Postembedding label was considerably more robust with

the EP1829Y antibody than with 6G9, although the general distribution of label was similar with both primary antibodies. A large fraction of dendritic spines from quick-fix material was immunolabeled with EP1829Y (Fig. 5A). Label was prominent in dendritic shafts, and was occasionally also found in presynaptic axon terminals (Fig. 5B,C). Although label was present near the synaptic specialization, much of the label in spines lay deep within the cytoplasm, often associated with filamentous material (Fig. 5B–E). Synapse-associated gold particles near the lateral border of the PSD commonly lay very close to the postsynaptic membrane, whereas those close to the middle of the synapse were often distant from the membrane (Fig. 5B,D).

Delay-fix material exhibited strong synaptic label (Fig. 5F,G). Label was also prominent over the characteristic electron-dense blobs (arrows in Fig. 5F,G). This label covered the entire dense region, in contrast to the pattern seen in pre-embedding, where label was mainly confined to the exterior surface of the blob (cf. Fig. 3B); apparently these electron-dense structures excluded primary antibody during pre-embedding immune processing, in a manner reminiscent of the PSD. Immunolabeled dense blobs were occasionally also seen in rapidly fixed material, but were detected in only three of nine animals studied. We speculate that this reflects either that the region of hippocampus studied was exceptionally active at the time of fixation, or that there was poor local access to fixative in the region examined.

For quantitative analysis, we analyzed randomly selected images containing postsynaptic spines with clear-cut postsynaptic membrane from the six rats lacking CaMKII-positive blobs, and measured “axodendritic” and “lateral” distributions of CaMKII (see Materials and Methods, and Valtschanoff and Weinberg (2001) for details of data analysis). More spines were immunolabeled with the EP1829Y antibody than with 6G9, with more particles/synapse, but the distribution of particles was very similar for the two antibodies, although they have slightly different specificities (EP1829Y is reported to recognize all CaMKII isoforms, whereas 6G9 recognizes only CaMKIIα). When attention was confined to particles within 0–70 nm of the postsynaptic membrane, and <1.1 normalized lateral units away from the center of the PSD (and thus plausibly related to the PSD), the mean axodendritic position of 6G9 was 35 ± 1 nm (n = 176), versus 36 ± 1 nm (n = 257) for EP1829Y ($P > 0.7$, two-sided t-test), and the mean normalized lateral position of 6G9 was 0.50 ± 0.02 (n = 176), versus 0.51 ± 0.02 (n = 257) for EP1829Y ($P > 0.5$). While consistent with published evidence that the large majority of CaMKII in forebrain homogenate and in purified PSDs from forebrain is the α isoform (Bennett et al., 1983; Miller and Kennedy, 1985), our result also suggests that CaMKIIβ associated with the PSD is organized similarly to the α isoform, at least in the spine head. As the two distributions appeared virtually identical, we pooled data from both antibodies to improve the accuracy and robustness of the results. By analyzing the axodendritic distribution pattern, we found that whereas labeling was present, it did not concentrate within the core of the PSD (Fig. 6A). Instead, CaM-KII labeling peaked 35–45 nm inside the postsynaptic membrane, at the cytoplasmic fringe of the PSD; a smaller peak at ∼25 nm revealed a comparatively modest accumulation of antigen within the PSD core.

To test our subjective impression that label near the middle of the synapse seemed to avoid the vicinity of the postsynaptic membrane, we measured lateral positions and computed the

"normalized lateral distribution" tangentially along the synapse for these two synapse-related pools (see Materials and Methods for details). The lateral distribution of particles lying within the PSD "core" (considering only particles lying 0–25 nm from the plasma membrane) differed significantly from that of particles from the "cytoplasmic fringe," lying 26–70 nm from the membrane ($P < 0.001$, Kolmogorov-Smir-nov test). CaMKII within the PSD core concentrated at the periphery of the synapse (median "normalized lateral position" of 0.65, $n = 155$), whereas the main pool of label lying at the cytoplasmic fringe was more uniformly distributed along the synapse, concentrating in a more central region (median normalized lateral position of 0.48, $n = 295$; $P < 0.01$, Wilcoxon rank sum test; Fig. 6B).

To further assess possible differences between these two pools, we compared the axodendritic distribution of "peripheral" (0.6–1.1, $n = 257$) and "central" (normalized lateral position 0–0.5, $n = 325$) immunogold particles lying within ±100 nm of the postsynaptic membrane (Fig. 6C). As predicted, the peak of the peripheral labeling was only 10–20 nm from the membrane, ∼25 nm closer than the peak of central labeling. Because these data include several sources of noise, it is likely that they underestimate the true differences between CaMKII lying at peripheral and central sectors of the synapse.

We conclude that when precautions are taken to minimize fixation delay and the associated hypoxic/ischemic stress, only a relatively modest fraction of the CaMKII within the dendritic spine lies inside the PSD, and this pool concentrates at its periphery.

Discussion

Technical issues

Although conceptually a simple question, in practice it is challenging to estimate the distribution of CaMKII in different neuronal compartments within the living brain. Early studies (Kennedy et al., 1983; Goldenring et al., 1984; Kelly et al., 1984) found very high levels of CaMKII within the PSD fraction; this result has since been replicated by many labs using similar methods. However, Suzuki and colleagues found that the concentration of CaMKII in the PSD fraction was considerably reduced if the rat brain was quickly frozen in liquid nitrogen immediately after decapitation (Suzuki et al., 1994). Several other biochemical studies confirmed that CaMKII may translocate quickly from supernatant to pellet, or from homogenate into the PSD fraction, after ischemia (Aronowski et al., 1992; Hu and Wieloch, 1995; Kolb et al., 1995; Hu et al., 1998; Domańska-Janik et al., 1999). The biochemical evidence for ischemia-induced translocation into synapses must also be treated with caution, because hypoxic/ischemic stress can also cause CaMKII to aggregate into ∼100-nm blobs, which may cofractionate with the PSD (Dosemeci et al., 2000), but ultrastructural study confirms its translocation into the anatomical PSD (Hu et al. 1998; Tao-Cheng et al., 2007).

Although the phenomenon has been linked to brain ischemia, the actual trigger for the dramatic reorganization of CaMKII remains unclear, and might reflect hypoxia, glucose/ATP depletion, excessive activation of glutamate receptors, and/or elevated intradendritic Ca^{2+} (Dosemeci et al., 2001; Tao-Cheng et al., 2001, 2002); in this manuscript we therefore use the noncommittal term "hypoxic/ischemic stress." The phenomenon has

been best demonstrated in pathological models, but a milder form of this reorganization may be physiologically significant. Indeed, synaptic CaMKII may be highly dynamic in vivo, shuttling in and out of the PSD depending on levels of synaptic activation, although presumably to a lesser degree than after decapitation.

In the present work, we employed quantitative immunocytochemistry on sections cut from fixed brains, to avoid difficulties associated with biochemical fractionation. Based on the onset of rigor in our quick-fix material, we estimate a delay of <60 seconds after the cessation of respiration, before fixative caused enough cross-linking to anchor neuronal CaMKII. Although even rapid chemical fixation is far slower than is possible with high-pressure freezing, this rapid freezing technique cannot be performed on intact brain without severe hypoxia and mechanical trauma. The hypoxia sustained by our quick-fix material, though exceeding that ordinarily encountered by an adult rodent, was far milder than the 15 minutes of experimental ischemia used in Hu et al. (1998), especially considering that our animals were under deep barbiturate anesthesia. Although our data from quick-fix material should be taken as an upper bound for the concentration of CaMKII in the PSD *in vivo*, the rather modest shifts we found in CaMKII organization after control experiments that included 5 minutes of delay before fixation suggest that the quick-fix estimates of antigen location are not severely impacted by the delay arising from chemical fixation, and may be close to the organization in living brain. However, because our data rely on averaged results, they likely fail to detect the extent of synapse-to-synapse variability (which may be considerable; see Fera et al., 2012).

Cytoplasmic distribution of CaMKII

By using pre-embedding immunogold to provide a high-resolution quantitative estimate, the present results document a high concentration of CaMKII in dendritic shafts; in fact, after rapid fixation, CaMKII labeling was denser in shafts than in dendritic spines. This is a higher shaft-to-spine ratio than reported in previous live-cell imaging work (Otmakhov et al. 2004), perhaps reflecting differences between slice culture and intact brain. The CaMKII translocation seen in response to ischemic/hypoxic stress can be viewed as two distinct processes: a flow of CaMKII from shaft to spine head (as previously visualized by in vitro imaging experiments), and local movement within the spine head over distances of ∼100–200 nm.

CaMKII in dendritic shafts may play a structural role. It is known that stabilization of the dendritic arbor during development coincides with the period of increasing CaMKII levels, whereas overexpression of CaMKII can induce precocious maturation of the dendritic arbor (Wu and Cline, 1998; Zou and Cline, 1999). The underlying mechanism is not entirely clear, although CaMKII can bundle F-actin, which could explain its role in stabilizing dendrites (Okamoto et al., 2004, 2007). Unlike dendrites, spines exhibit considerable actin-mediated morphological plasticity even in the adult (Zito et al., 2004; Honkura et al., 2008), perhaps reflecting the lower concentration of CaMKII in spines.

CaMKII at the PSD

Pre-embedding methods often fail to label synaptic proteins; it is generally thought that the dense matrix of the PSD blocks antibody access. Postembedding immunogold labeling is less sensitive than pre-embedding, but besides providing excellent spatial accuracy, post-embedding techniques yield an unbiased signal unaffected by differential antibody access to specific cellular compartments (Valtschanoff and Weinberg 2001). We therefore used postembedding immunogold to determine the relationship of CaMKII to the PSD, finding that it concentrated ∼40 nm from the postsynaptic membrane. Should this locus be considered part of the PSD? Recent data from electron tomography reveals a dense matrix in a ∼25-nm zone directly apposed to the plasma membrane, coated by a progressively attenuated fringe of electron-dense material that extends filaments into the cytoplasm of the spine (Burette et al, 2012); accordingly, we consider this zone to be distinct from the PSD core, and here refer to it as the cytoplasmic fringe of the PSD. Results from a previous immunogold study on biochemically isolated PSDs (Petersen et al., 2003) are generally consistent with ours, as is a recent high-resolution electron tomographic study (Fera et al., 2012) if one bears in mind that the disruption inherent to the PSD isolation in those studies likely caused the loss preferentially of CaMKII that lay farthest from the postsynaptic membrane. CaMKII lying this far from the membrane is poorly positioned to interact with glutamate receptors inserted into the membrane, but could (for example) interact with F-actin to help mediate activity-dependent cytoskeletal reorganization.

Our data suggest that most of the CaMKII in dendritic spines lies outside the PSD, and even that fraction clearly associated with the PSD tends to avoid the zone close to the plasma membrane. The pool of CaMKII embedded within the core of the PSD concentrated at its lateral edge. We speculate that this “lateral” pool might have a distinct function. Although the mechanistic details that underlie the coupling of CaMKII activation to LTP remain unclear, it is now generally agreed that LTP involves expression of new AMPA receptors. Current evidence (Kennedy et al., 2010) suggests that these receptors are inserted just lateral to the PSD; a pool of CaMKII at the periphery of the synapses would be ideally positioned to help mediate this task. This pool of CaMKII might serve to phosphorylate Stargazin and related scaffold proteins, thus diffusionally trapping AMPA receptors in the PSD (Opazo et al., 2010; Shin et al., 2012). In addition, recent work shows that the association of CaMKII with NMDA receptors is essential for LTP-driven stabilization of new spines (Hill and Zito, 2013), and F-actin filaments (the dominant element of the spinoskeleton) concentrate at the lateral edge of the PSD (Burette et al. 2012). Interactions besides those directly targeting ionotropic receptors may also be functionally relevant (Oh et al., 2004; Newpher and Ehlers, 2009; Dosemeci and Jaffe, 2010). For example, type I metabotropic glutamate receptors, which concentrate at the edge of the PSD (Baude et al., 1993), bind to Homer; by phosphorylating Homer (as has been documented in cerebellum (Mizutani et al., 2008), CaM-KII in this peripheral pool might regulate its coupling to target molecules also in the hippocampus.

Supplementary Material

Refer to Web version on PubMed Central for supplementary material.

Acknowledgments

We thank Susan Burette and Kristen D. Phend for histological assistance; Alain Burette for confocal analysis of double-labeling immunofluorescence; and Alain Burette, Ayse Dosemeci, Johannes Hell, and Sridhar Raghavachari for comments on the manuscript text.

Grant sponsor: National Institutes of Health; grant numbers: P01 NS44306 (to M.B.K.) and R01 NS35527 (to R.J.W.).

Literature Cited

Aronowski J, Grotta JC, Waxham MN. Ischemia-induced translocation of Ca^{2+}/calmodulin-dependent protein kinase II: potential role in neuronal damage. J Neuro-chem. 1992; 58:1743–1753.

Barria A, Malinow R. NMDA receptor subunit composition controls synaptic plasticity by regulating binding to CaMKII. Neuron. 2005; 48:289–301. [PubMed: 16242409]

Barria A, Muller D, Derkach V, Griffith LC, Soderling TR. Regulatory phosphorylation of AMPA-type glutamate receptors by CaM-KII during long-term potentiation. Science. 1997; 276:2042–2045. [PubMed: 9197267]

Baude A, Nusser Z, Roberts JD, Mulvihill E, McIlhinney RA, Somogyi P. The metabotropic glutamate receptor (mGluR1 α) is concentrated at perisynaptic membrane of neuronal subpopulations as detected by immunogold reaction. Neuron. 1993; 11:771–787. [PubMed: 8104433]

Bayer KU, Lohler J, Schulman H, Harbers K. Developmental expression of the CaM kinase II isoforms: ubiquitous γ- and δ-CaM kinase II are the early isoforms and most abundant in the developing nervous system. Brain Res Mol Brain Res. 1999; 70:147–154. [PubMed: 10381553]

Bennett MK, Erondu NE, Kennedy MB. Purification and characterization of a calmodulin-dependent protein kinase that is highly concentrated in brain. J Biol Chem. 1983; 258:12735–12744. [PubMed: 6313675]

Burette AC, Lesperance T, Crum J, Martone M, Volkmann N, Ellisman MH, Weinberg RJ. Electron tomographic analysis of synaptic ultrastructure. J Comp Neurol. 2012; 520:2697–2711. [PubMed: 22684938]

Burgin KE, Waxham MN, Rickling S, Westgate SA, Mobley WC, Kelly PT. *In situ* hybridization histochemistry of Ca^{2+}/calmodulin-dependent protein kinase in developing rat brain. J Neurosci. 1990; 10:1788–1798. [PubMed: 2162385]

Chen X, Vinade L, Leapman RD, Petersen JD, Nakagawa T, Phillips TM, Sheng M, Reese TS. Mass of the postsynaptic density and enumeration of three key molecules. Proc Natl Acad Sci U S A. 2005; 102:11551–11556. [PubMed: 16061821]

Domańska-Janik K, Zalewska T, Zablocka B, Ostrowski J. Ischemia-induced modifications of protein components of rat brain postsynaptic densities. Neurochem Int. 1999; 34:329–336. [PubMed: 10372919]

Dosemeci A, Jaffe H. Regulation of phosphorylation at the postsynaptic density during different activity states of Ca^{2+}/calmodulin-dependent protein kinase II. Biochem Biophys Res Commun. 2010; 391:78–84. [PubMed: 19896464]

Dosemeci A, Reese TS, Petersen J, Tao-Cheng JH. A novel particulate form of Ca^{2+}/calmodulin-dependent protein kinase II in neurons. J Neurosci. 2000; 20:3076–3084. [PubMed: 10777771]

Dosemeci A, Tao-Cheng JH, Vinade L, Winters CA, Pozzo-Miller L, Reese TS. Glutamate-induced transient modification of the postsynaptic density. Proc Natl Acad Sci U S A. 2001; 98:10428–10432. [PubMed: 11517322]

Erondu NE, Kennedy MB. Regional distribution of type II Ca^{2+}/calmodulin-dependent protein kinase in rat brain. J Neurosci. 1985; 5:3270–3277. [PubMed: 4078628]

Fera A, Dosemeci A, Sousa AA, Yang C, Leapman RD, Reese TS. Direct visualization of CaMKII at postsynaptic densities by electron microscopy tomography. J Comp Neurol. 2012; 520:4218–4225. [PubMed: 22627922]

Goldenring JR, McGuire JS Jr, DeLorenzo RJ. Identification of the major postsynaptic density protein as homologous with the major calmodulin-binding subunit of a calmodulin-dependent protein kinase. J Neurochem. 1984; 42:1077–1084. [PubMed: 6699638]

Halt AR, Dallapiazza RF, Zhou Y, Stein IS, Qian H, Juntti S, Wojcik S, Brose N, Silva AJ, Hell JW. CaMKII binding to GluN2B is critical during memory consolidation. EMBO J. 2012; 31:1203–1216. [PubMed: 22234183]

Hill TC, Zito K. LTP-induced long-term stabilization of individual nascent dendritic spines. J Neurosci. 2013; 33:678–686. [PubMed: 23303946]

Honkura N, Matsuzaki M, Noguchi J, Ellis-Davies GC, Kasai H. The subspine organization of actin fibers regulates the structure and plasticity of dendritic spines. Neuron. 2008; 57:719–729. [PubMed: 18341992]

Hu BR, Wieloch T. Persistent translocation of Ca^{2+}/cal-modulin-dependent protein kinase II to synaptic junctions in the vulnerable hippocampal CA1 region following transient ischemia. J Neurochem. 1995; 64:277–284. [PubMed: 7798923]

Hu BR, Park M, Martone ME, Fischer WH, Ellisman MH, Zivin JA. Assembly of proteins to postsynaptic densities after transient cerebral ischemia. J Neurosci. 1998; 18:625–633. [PubMed: 9425004]

Kelly PT, McGuinness TL, Greengard P. Evidence that the major postsynaptic density protein is a component of a Ca^{2+}/calmodulin-dependent protein kinase. Proc Natl Acad Sci U S A. 1984; 81:945–949. [PubMed: 6583689]

Kennedy MB, Bennett MK, Erondu NE. Biochemical and immunochemical evidence that the “major postsynaptic density protein” is a subunit of a calmodulin-dependent protein kinase. Proc Natl Acad Sci U S A. 1983; 80:7357–7361. [PubMed: 6580651]

Kennedy MJ, Davison IG, Robinson CG, Ehlers MD. Syn-taxin-4 defines a domain for activity-dependent exocytosis in dendritic spines. Cell. 2010; 141:524–535. [PubMed: 20434989]

Kharazia VN, Weinberg RJ. Immunogold localization of AMPA and NMDA receptors in somatic sensory cortex of albino rat. J Comp Neurol. 1999; 412:292–302. [PubMed: 10441757]

Kolb SJ, Hudmon A, Waxham MN. Ca^{2+}/calmodulin kinase II translocates in a hippocampal slice model of ischemia. J Neurochem. 1995; 64:2147–2156. [PubMed: 7722499]

Lee SJ, Escobedo-Lozoya Y, Szatmari EM, Yasuda R. Activation of CaMKII in single dendritic spines during long-term potentiation. Nature. 2009; 458:299–304. [PubMed: 19295602]

Lisman J, Schulman H, Cline H. The molecular basis of CaMKII function in synaptic and behavioural memory. Nat Rev Neurosci. 2002; 3:175–190. [PubMed: 11994750]

Lisman J, Yasuda R, Raghavachari S. Mechanisms of CaMKII action in long-term potentiation. Nat Rev Neurosci. 2012; 13:169–182. [PubMed: 22334212]

Lledo PM, Hjelmstad GO, Mukherji S, Soderling TR, Malenka RC, Nicoll RA. Calcium/calmodulin-dependent kinase II and long-term potentiation enhance synaptic transmission by the same mechanism. Proc Natl Acad Sci U S A. 1995; 92:11175–11179. [PubMed: 7479960]

Miller SG, Kennedy MB. Distinct forebrain and cerebellar isozymes of type II Ca^{2+}/calmodulin-dependent protein kinase associate differently with the postsynaptic density fraction. J Biol Chem. 1985; 260:9039–9046. [PubMed: 4019461]

Mizutani A, Kuroda Y, Futatsugi A, Furuichi T, Mikoshiba K. Phosphorylation of Homer3 by calcium/calmodulin-dependent kinase II regulates a coupling state of its target molecules in Purkinje cells. J Neurosci. 2008; 28:5369–5382. [PubMed: 18480293]

Newpher TM, Ehlers MD. Spine microdomains for post-synaptic signaling and plasticity. Trends Cell Biol. 2009; 19:218–227. [PubMed: 19328694]

Oh JS, Manzerra P, Kennedy MB. Regulation of the neuron-specific Ras GTPase-activating protein, synGAP, by Ca^{2+}/calmodulin-dependent protein kinase II. J Biol Chem. 2004; 279:17980–17988. [PubMed: 14970204]

Okamoto K, Nagai T, Miyawaki A, Hayashi Y. Rapid and persistent modulation of actin dynamics regulates post-synaptic reorganization underlying bidirectional plasticity. Nat Neurosci. 2004; 7:1104–1112. [PubMed: 15361876]

Okamoto K, Narayanan R, Lee SH, Murata K, Hayashi Y. The role of CaMKII as an F-actin-bundling protein crucial for maintenance of dendritic spine structure. Proc Natl Acad Sci U S A. 2007; 104:6418–6423. [PubMed: 17404223]

Opazo P, Labrecque S, Tigaret CM, Frouin A, Wiseman PW, De Koninck P, Choquet D. CaMKII triggers the diffusional trapping of surface AMPARs through phosphorylation of stargazin. Neuron. 2010; 67:239–252. [PubMed: 20670832]

Otmakhov N, Tao-Cheng JH, Carpenter S, Asrican B, Dosemeci A, Reese TS, Lisman J. Persistent accumulation of calcium/calmodulin-dependent protein kinase II in dendritic spines after induction of NMDA receptor-dependent chemical long-term potentiation. J Neurosci. 2004; 24:9324–9331. [PubMed: 15496668]

Petersen JD, Chen X, Vinade L, Dosemeci A, Lisman JE, Reese TS. Distribution of postsynaptic density (PSD)-95 and Ca^{2+}/calmodulin-dependent protein kinase II at the PSD. J Neurosci. 2003; 23:11270–11278. [PubMed: 14657186]

Petralia RS, Sans N, Wang YX, Wenthold RJ. Ontogeny of postsynaptic density proteins at glutamatergic synapses. Mol Cell Neurosci. 2005; 29:436–452. [PubMed: 15894489]

Phend KD, Rustioni A, Weinberg RJ. An osmium-free method of Epon embedment that preserves both ultra-structure and antigenicity for post-embedding immunocy-tochemistry. J Histochem Cytochem. 1995; 43:283–292. [PubMed: 7532656]

Sato T. A modified method for lead staining of thin sections. J Electron Microsc (Tokyo). 1968; 17:158–159. [PubMed: 4177281]

Shin SM, Zhang N, Hansen J, Gerges NZ, Pak DT, Sheng M, Lee SH. GKAP orchestrates activity-dependent postsynaptic protein remodeling and homeostatic scaling. Nat Neurosci. 2012; 15:1655–1666. [PubMed: 23143515]

Sik A, Hajos N, Gulacsi A, Mody I, Freund TF. The absence of a major Ca^{2+} signaling pathway in GABAergic neurons of the hippocampus. Proc Natl Acad Sci U S A. 1998; 95:3245–3250. [PubMed: 9501248]

Soderling TR. CaM-kinases: modulators of synaptic plasticity. Curr Opin Neurobiol. 2000; 10:375–380. [PubMed: 10851169]

Suzuki T, Okumura-Noji K, Tanaka R, Tada T. Rapid translocation of cytosolic Ca^{2+}/calmodulin-dependent protein kinase II into postsynaptic density after decapitation. J Neurochem. 1994; 63:1529–1537. [PubMed: 7931307]

Tao-Cheng JH, Vinade L, Smith C, Winters CA, Ward R, Brightman MW, Reese TS, Dosemeci A. Sustained elevation of calcium induces Ca^{2+}/calmodulin-dependent protein kinase II clusters in hippocampal neurons. Neuroscience. 2001; 106:69–78. [PubMed: 11564417]

Tao-Cheng JH, Vinade L, Pozzo-Miller LD, Reese TS, Dosemeci A. Calcium/calmodulin-dependent protein kinase II clusters in adult rat hippocampal slices. Neuroscience. 2002; 115:435–440. [PubMed: 12421609]

Tao-Cheng JH, Gallant PE, Brightman MW, Dosemeci A, Reese TS. Structural changes at synapses after delayed perfusion fixation in different regions of the mouse brain. J Comp Neurol. 2007; 501:731–740. [PubMed: 17299754]

Valtschanoff JG, Weinberg RJ. Laminar organization of the NMDA receptor complex within the postsynaptic density. J Neurosci. 2001; 21:1211–1217. [PubMed: 11160391]

Wu GY, Cline HT. Stabilization of dendritic arbor structure in vivo by CaMKII. Science. 1998; 279:222–226. [PubMed: 9422694]

Zito K, Knott G, Shepherd GM, Shenolikar S, Svoboda K. Induction of spine growth and synapse formation by regulation of the spine actin cytoskeleton. Neuron. 2004; 44:321–334. [PubMed: 15473970]

Zou DJ, Cline HT. Postsynaptic calcium/calmodulin-dependent protein kinase II is required to limit elaboration of presynaptic and postsynaptic neuronal arbors. J Neurosci. 1999; 19:8909–8918. [PubMed: 10516310]

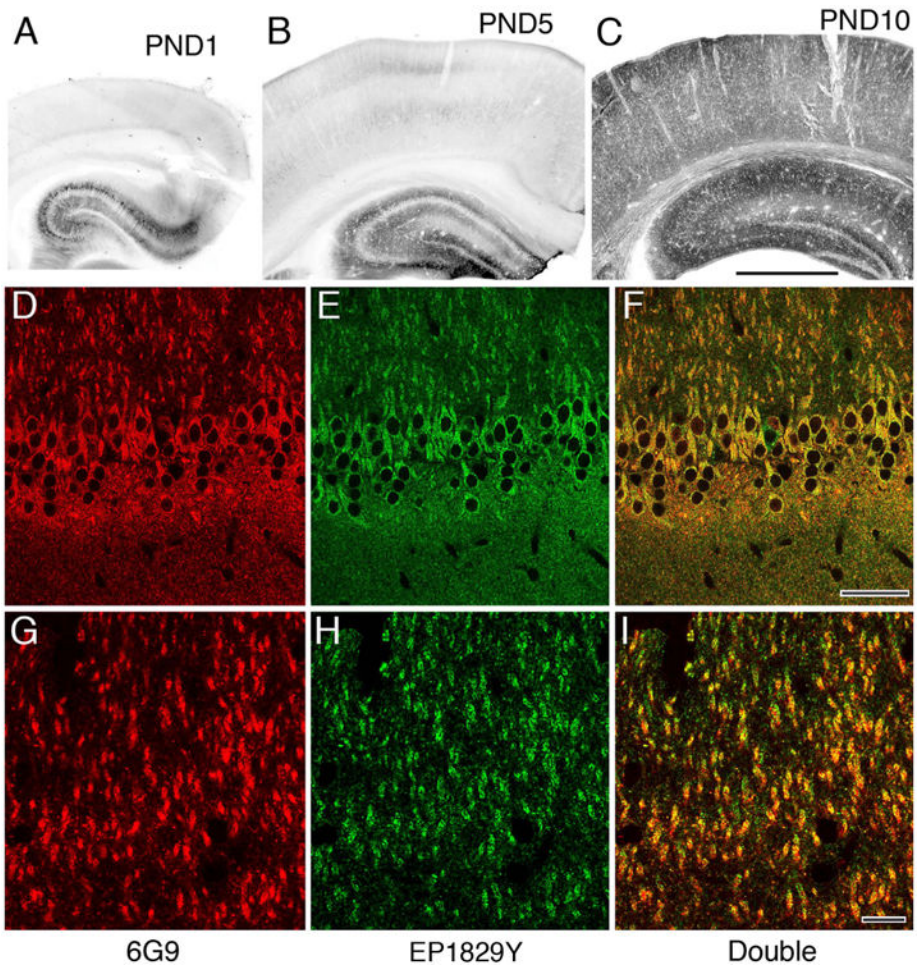

Figure 1.

Characterization of primary antibodies used for immunohistochemistry. **A,B**: Early in postnatal development immunoperoxidase staining with the 6G9 antibody is weak in hippocampus (largely restricted to a few well-stained pyramidal cells), and nearly absent from overlying cerebral cortex. **C**: By PND 10, staining is widespread in hippocampus, and has become prominent in cortex. **D–I**: Immunofluorescence staining in adult CA1 for the 6G9 antibody (red channel, left) displays extensive colocalization with staining for the Origene antibody (green channel, middle), as confirmed by the yellow images on right (both channels merged). (A magenta–green version is provided as Supplementary Fig. 1 for the assistance of color-blind readers). Scale bar = 1 mm in C (applies to A–C); 50 μm in F (applies to D–F); 10 μm in I (applies to G–I). [Color figure can be viewed in the online issue, which is available at wileyonlinelibrary.com].

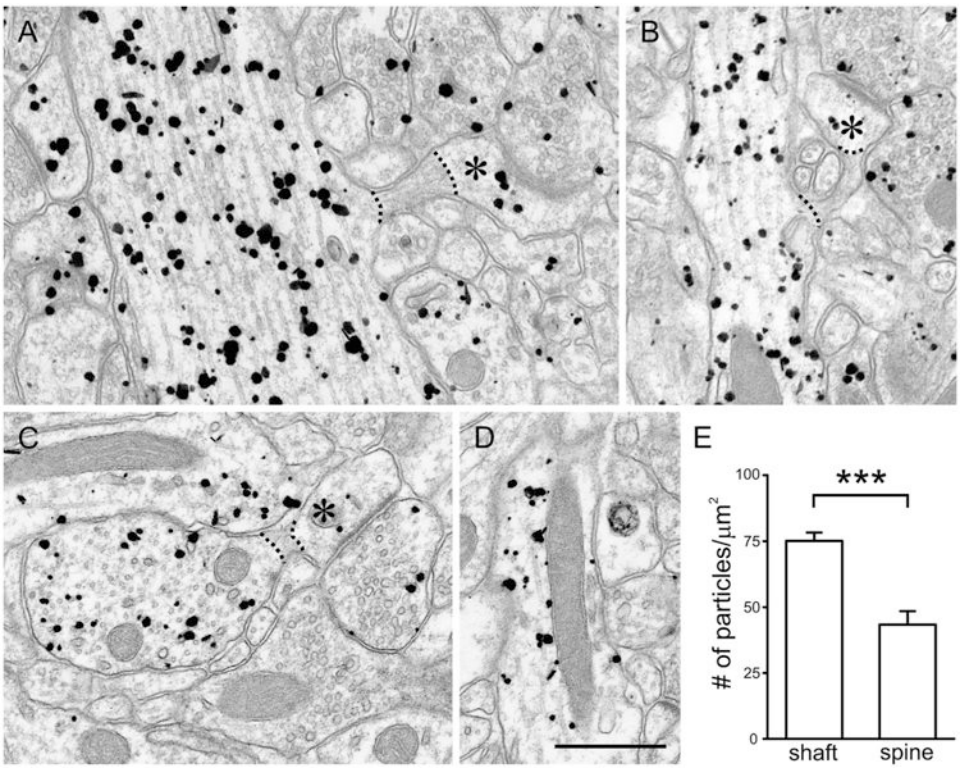

Figure 2.

Pre-embedding immunogold labeling in stratum radiatum of CA1 after quick fixation. Labeling is found in both dendritic shafts and spines of pyramidal neurons; labeling is also visible in presynaptic terminals. **A,B**: Dendritic shafts seem to label more strongly than the spine heads in continuity with them (asterisks). **C,D**: Within the shafts, labeling is found in association with microtubules (C) and mitochondria (D). For quantitative analysis, we analyzed micrographs that included both a parent dendrite and its spines in the same plane of section (to ensure that we compared CaMKII labeling from the same region of the same neurons), and compared labeling density in den-drites and spine heads; the spine neck (identifiable by multiple features, including its increased electron density and abundance of actin filaments) was ignored (see dotted lines in A–C). **E**: Labeling density was significantly higher in shafts than in spine heads (***$P < 0.001$; *t*-test). Scale bar = 500 nm in D (applies to A–D).

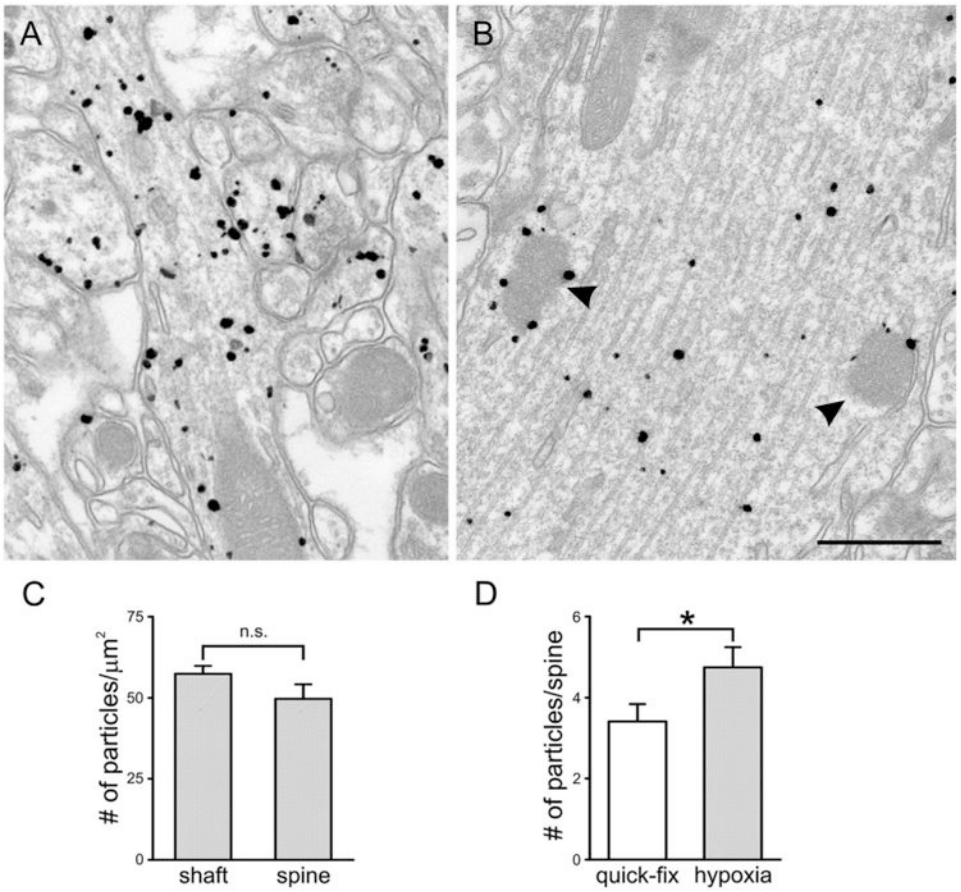

Figure 3.

Pre-embedding immunogold labeling in stratum radiatum after delayed fixation. **A**: CaMKII labeling is found both in dendritic shafts and spines; labeling in spines seems stronger than after quick fixation. **B**: Characteristic electron-dense spheroids in the dendritic shaft (arrowheads) are decorated with CaMKII labeling. To determine whether CaMKII reorganizes rapidly with hypoxia, spines and their parent shafts from brains fixed after 5-minute perfusion with saline were analyzed as for quick-fix tissue. **C**: Unlike in the quick-fix tissue, labeling density in the delay-fix material was similar for shaft and spine heads (n.s., not significant). **D**: The total number of particles per spine head was significantly larger in delay-fix than quick-fix spines (*$P < 0.05$, *t*-test). Scale bar = 500 nm in B (applies to A,B).

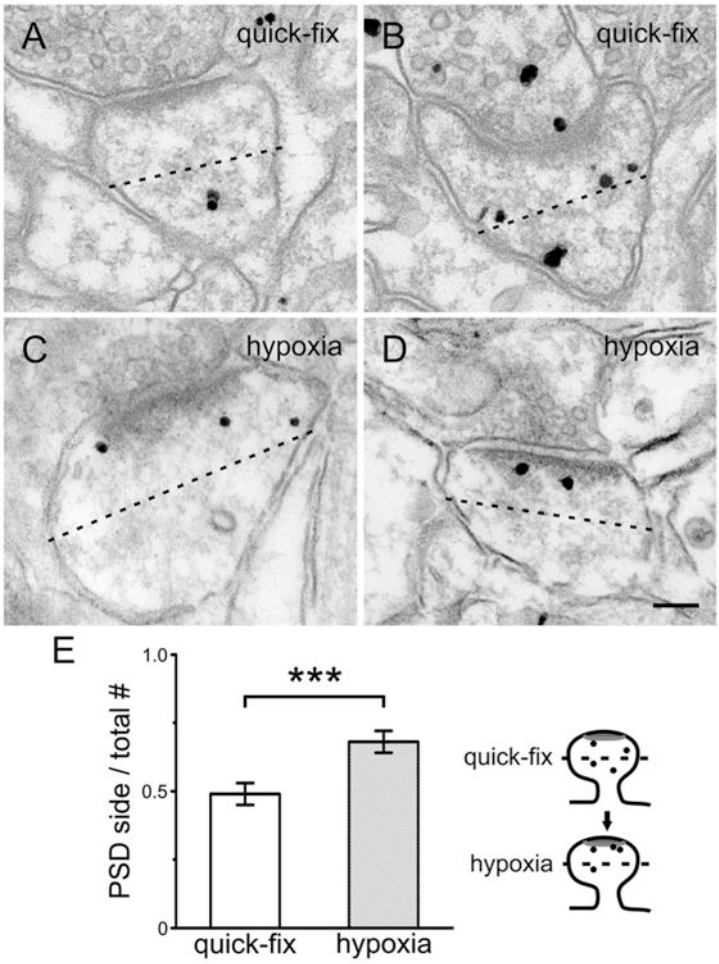

Figure 4.

Pre-embedding immunogold labeling in spines. **A–D**: After quick fixation (A,B), silver-enhanced gold particles seem to lie farther from the PSD than after delayed fixation (C,D). **E**: To test this impression, we bisected the spine head (dotted line) into a "distal" half including the PSD, and a "proximal" half facing the parent dendrite (see cartoon on right), and measured the relative distributions of CaM-KII in 49 quick-fix and 54 delay-fix spines (computing the numbers of particles on PSD side/total number of particles in the spine; 0.5 would correspond to an equal distribution). Delayed fixation caused translocation of CaMKII toward the PSD (***$P < 0.001$, *t*-test). Scale bar = 100 nm in D (applies to A–D).

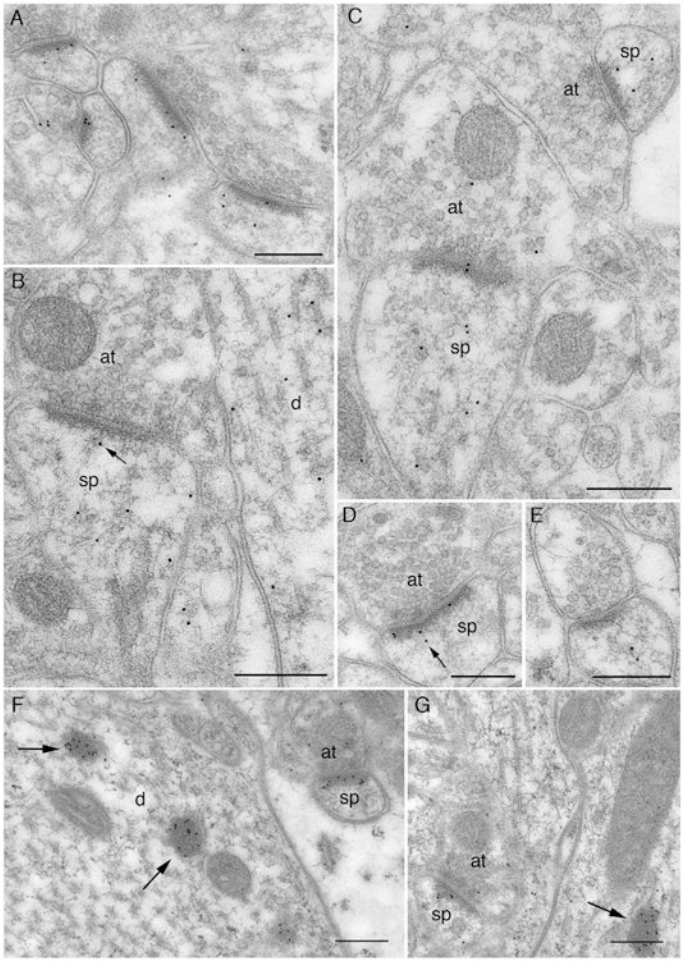

Figure 5.

Postembedding immunogold label for CaMKII using the EP1829Y antibody. A–E: Micrographs from quick-fixed material. F–G: From material that was perfused with saline for 5 minutes prior to fixation. **A**: General view of synaptic neuropil. Immunogold label (10-nm gold particles) is present in a large fraction of dendritic spines; much of this label is associated with the PSD. **B**: Label over axospinous synapse (left) is within the dendritic spine (sp), sparing the presynaptic axon terminal (at). One particle (arrow) is associated with filamentous material running from the PSD to the spine cytoplasm, whereas several other particles are in the matrix of the spine (perhaps associated with actin filaments). Label in the dendritic shaft (d) lies over microtubules and associated filaments. **C**: Axospinous synapse (left) contains both pre- and postsynaptic labeling. Label on the small asymmetric synapse (top right) is exclusively within the spine, lying away from the core of the PSD. **D**: Label over the spine runs along the length of the PSD. The two particles (arrow) associated with the tangentially defined “center” of the synapse lie farther from the plasma membrane than the particles closer to its edge. **E**: Label is associated with filamentous material in the spine core, and lies at a considerable distance from the synapse. **F**: Exuberant labeling over the PSD of a small dendritic spine profile. Heavily labeled electron-dense spheroids inside large dendritic shaft (arrows) superficially resemble nearby unlabeled mitochondria. **G**: Gold

particles near the center of the PSD lie close to the plasma membrane, whereas particles at the periphery lie farther from the membrane (contrast with D). Unlabeled mitochondria show more internal structure than the labeled dense spheroid (arrow). Abbreviations: at, axon terminal; d, dendritic shaft; sp, spine. Scale bar = 250 nm in A–G.

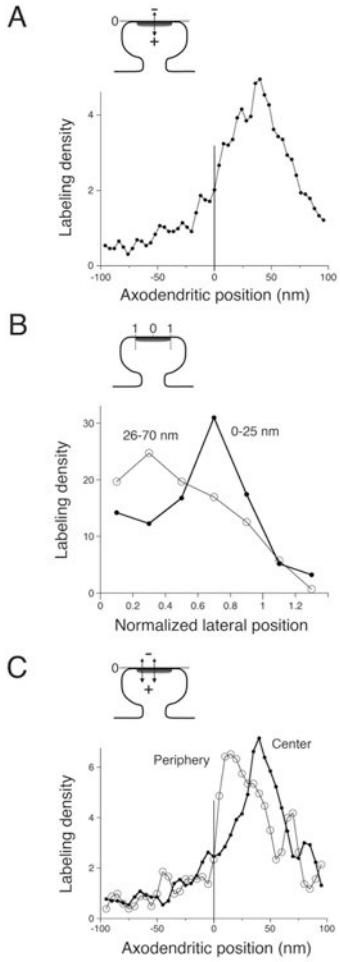

Figure 6.

Quantitative analysis of CaMKII distribution at the synapse, from quick-fix material. **A**: Labeling did not concentrate within the core of the PSD. Instead, the peak was ∼35–45 nm inside the postsynaptic membrane, at the cytoplasmic fringe of the PSD; a smaller peak at ∼25 nm indicates a relatively modest accumulation of antigen within the PSD core. Graph shows the relative density of labeling as a function of axodendritic position, based on measurements from 656 gold particles lying within the tangential limits of the synapse (normalized lateral position ≤1.1); data were smoothed by using a three-point moving weighted average. **B**: CaMKII within the "PSD core" pool (considering only particles between 0 nm and 25 nm from the postsynaptic membrane (n = 155)) concentrated near the lateral edge of the synapse (thick line). In contrast, for the main pool that lies at its cytoplasmic fringe (considering particles lying 26–70 nm inside the postsynaptic membrane [n = 295]), CaMKII concentrated in the central zone of the synapse (thin line). C: Graphs compare the axodendritic position of peripheral (normalized lateral position ≥ 0.6, n = 257 particles) and central (normalized lateral position ≤ 0.5, n = 325 particles) pools of label. The peripheral pool (thin line in graph) lay markedly closer to the plasma membrane than the central pool (thick line). Cartoons at top of each panel are schematic diagrams to illustrate "axodendritic" and "normalized lateral" measurements.

Table 1

Primary Antibodies

Antibody	Immunogen	Description	Source	Dilution
6G9	α-subunit of CaMKII	Mouse monoclonal	Mary B. Kennedy (Caltech)	1:1,000 (immunoperoxidase, immunofluorescence and pre-embedding immunogold); 1:100 (postembedding immunogold)
EP1829Y	A 15-amino acid sequence within amino acids 200–250 of human CaMKII	Rabbit monoclonal	OriGene (Rockville, MD); clone EP1829Y; cat. No. TA303876	1:800 (postembedding immunogold)